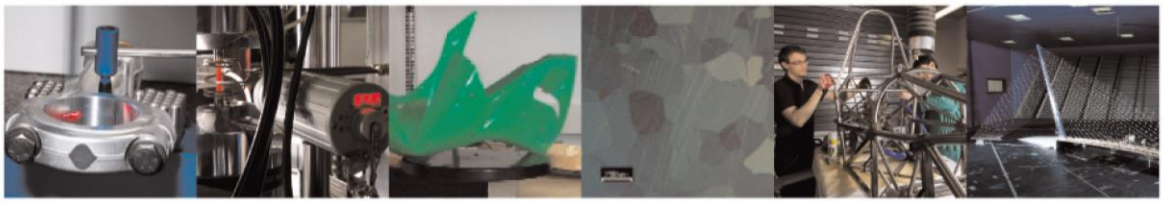

Energy saving opportunities in direct drive machine tool spindles

Albertelli, Paolo

This is a post-peer-review, pre-copyedit version of an article published in JOURNAL OF CLEANER PRODUCTION. The final authenticated version is available online at: http://dx.doi.org/10.1016/j.jclepro.2017.07.175]

DIPARTIMENTO DI MECCANICA ■ POLITECNICO DI MILANO
via G. La Masa, 1 ■ 20156 Milano ■ EMAIL (PEC): pecmecc@cert.polimi.it
http://www.mecc.polimi.it
Rev. 0

Energy saving opportunities in direct drive machine tool spindles

Paolo Albertelli[a,]

[a]*Department of Mechanical Engineering, Politecnico di Milano, Milan, Italy*

Abstract

The aim of the work is to carry out a comprehensive assessment of the energy saving opportunities linked to the introduction of direct drives solutions in machine tool spindle systems. Although there is a clear industrial trend towards the replacement of the traditional motor-transmission based spindle solutions, there is a lack of scientific studies focused on the associated energy-related aspects. For this purpose, two spindle units characterized by similar performances were analyzed from the energy consumption, losses and efficiency perspective. Empirical spindle system energy models were developed exploiting experimental tests performed on a motor test bench used for reproducing different machining conditions. The identified models were used to estimate the energy savings that can be achieved substituting the traditional gearbox-based solution with the novel direct-drive spindle. The analysis was carried out considering a realistic production scenario for the machine equipped with the analyzed spindle. It was demonstrated that about 7% of the energy absorbed by the overall machine can be saved and that this improvement accounts for the 147% of the requested cutting energy. For sake of generality, the analysis was repeated considering different production scenarios and ways of using the machine. It can be concluded that the achievable energy savings are even robust to the change of the executed machining operations.

Keywords: energy savings, energy modeling, spindle systems, direct drives

1. Introduction

Since manufacturing is one of the most energy demanding industrial sectors, institutions, universities, industrial organizations and companies, each one at different levels and with different roles, started tackling the challenging issues of using energy in a more efficient way. The European Commission, in order to fulfil the Worldwide greenhouse gas emission reduction target, delivered a directive for the eco-design of energy-related products ErP (EU (2009)) that establishes a common framework for the promotion of energy efficiency policies.

Email address: paolo.albertelli@polimi.it (Paolo Albertelli)

This framework is useful also for machine tools and production systems. CECIMO, the European Association of Machine Tool Industries, launched a self-regulation initiative (CECIMO (2009)) that supported machine tool builders for the first implementation of eco-oriented actions. Fraunhofer-IZM (2011) issued a preparatory study that identifies a set of best available/not yet available technologies (BAT/BNAT) that could be successfully used for reducing the consumed energy by machinery. Moreover, it was stated that the machine use phase is much more relevant, for what concerns the absorbed energy, than other phases (i.e. machine production, transportation and post-use), Jayal et al. (2010)). In this scenario, the International Organization for Standardization ISO released the first part of a more structured standard (ISO/DIS 14955-1) that is focused on methodologies for the energy efficient machine tools design, ISO (2014). Other parts of the standard (testing procedures) are under development.

In the last few years a great research effort has been done to make manufacturing more efficient. As observed in Yingjie (2014), energy savings in machine tools can be accomplished by a proper energy-oriented machine tool components design or by promoting a better machine usage, both in terms of machining strategy or process parameter selection. Neugebauer et al. (2011) tried to outline general principles for enhancing the efficiency in machine centres.

The awareness of the most power-demanding machine tool components is without doubts the starting point for conceiving further energy saving strategies. For this purpose, an energy assessment approach based on experimental measurements was generally preferred. A standardized methodology for the energy assessment of machine tool (under development in ISO (2016)) is now close to be released. Analyzing the the experimental measurements reported in several papers (i.e. Li et al. (2011)), it was found that almost every machine uses relevant amount of energy just for being ready to operate. This is mainly due to the auxiliary equipment typically installed on modern machines.

Although the experimental approach is helpful for a first rough energy analysis, the availability of energy models would be very useful for investigating potential energy savings. This opportunity stimulated the scientific community that conceived various modeling approaches, described by Zhou et al. (2016) in their review paper.

Gutowski et al. (2006) applied the Exergy analysis to manufacturing. A theoretical reverse trend between specific energy consumption (SEC energy per unit of processed material) and the material removal rate MRR was found. The SEC was also used for comparing different machining processes. Gtze et al. (2012) proposed a methodology for modeling the energy flows and devising energy savings in machine tools. Yang et al. (2016) proposed a learning-based modeling approach that allows analyzing the effect of cutting parameters on energy consumption. He et al. (2012) developed a technique for estimating the machine energy consumption directly analyzing the NC code. It was observed that the presented methodologies, due to the introduced approximations, are not useful in many interesting cases. For this reason, empirical approaches or approaches that combine empirical and analytical methodologies are preferable. For instance, Diaz et al. (2009) developed a simple model for estimating the

consumed energy: a power contribution linked to the machine, measured when it is performing air cutting, and a term connected to the process were considered. Kara and Li (2011) proposed an empirical energy modeling that describes the relationships between the SEC and the main cutting parameters in turning. Draganescu et al. (2003) extended the study to milling machines. Balogun and Mativenga (2013) developed an empirical machine power model that consider the MRR as the main process-related quantity. Despite the spindle system is one of the most important machine tool components, in many researches it was modelled in a very simple way: for instance Mativenga and Rajemi (2011) proposed a model that considers exclusively the friction losses at different spindle speeds. Only few works that deal with machine tool energy consumption proposed more complex models for this component (i.e. (Borgia et al., 2016)).

Since it was demonstrated that energy can be saved through a proper cutting parameters selection (Diaz et al. (2009)), machine energy models have been used for the optimization of the machining conditions. The first research works were focused on turning. For instance, Velchev et al. (2014) proposed a methodology for modelling and minimizing the SEC. Rajemi et al. (2010) dealt with the energy footprint minimization. For that purpose, they developed an energy model that considers the wear of the tool and the energy required for producing the inserts. Yi et al. (2015) worked on a multi-objective parameter optimization in turning where the absorbed energy and the surface finishing were simultaneously considered. Campatelli et al. (2014) adopted the response surface methodology for minimizing the power consumption in milling. Kant and Sangwan (2014) exploited a similar approach for optimizing both the absorbed energy and the surface quality. Albertelli et al. (2016) proposed a generalized multi-parameter energy optimization approach based on a combined empirical-analytical model suitable for milling applications. Li et al. (2014) experimentally demonstrated that both low energy consumption and high production rates can be simultaneously achieved by selecting the right cutting parameters. Yan and Li (2013) presented a multi-objective optimization methodology that opportunely weights energy consumption, process-rate and the quality of the machined parts. Wang et al. (2014) used a genetic algorithm for the above described optimization while Hanafi et al. (2012) adopted the grey relationship theory and the Taguchi approach.

Much research effort was also dedicated to the definition of specific energy-oriented machining strategies, Aramcharoen and Mativenga (2014). For instance, Newman et al. (2012) showed that energy consumption can be considered an additional criteria in process planning. Pavanaskar et al. (2015) demonstrated that a proper tool-path definition policy can be used for minimizing the energy consumption. Huang and Ameta (2014) developed a first rough tool for estimating the energy linked to the part production. Borgia et al. (2016) developed a simulation approach for predicting and minimizing the energy consumption during general milling operations. Altıntaş et al. (2016) used the response surface methodology for finding the machining strategy that assures the minimization of the consumed energy. Guo et al. (2015) developed an operation-mode simulation approach that can be used to simultaneously opti-

mize, from the energy perspective, the tool path and the cutting parameters in turning.

Although the results of these researches demonstrated that appreciable energy savings can be achieved, the efficiency enhancement of machine tool components remains one of the most profitable ways for promoting sustainability in manufacturing. Several studies (i.e. Li et al. (2013)) focused on the reduction of the electric power absorbed when the machine is ready-to-operate were carried out. A relevant share of the energy is typically associated to cooling systems and hydraulic units. Some research projects dealt with the efficiency improvement of such systems. For instance, Brecher et al. (2012) analyzed two cooling systems from the energy consumption perspective: one that is based on state-of-art technology and another one equipped with an optimized solution. (Brecher et al., 2017) carried out a similar analysis on hydraulic units. In this study, the eco-efficient hydraulic units (i.e. equipped with a pressure booster or with an inverter coupled to an axial piston pump and accumulators) were compared to solutions based on BAT. Even machine tool auxiliary equipment suppliers autonomously developed their own eco-solutions: in some cases, quite relevant energy savings were achieved.

Focusing solely on energy consumption of machine auxiliaries is without doubts a too limiting approach. In fact, other groups of components can play a relevant role in the total consumption determination. This was demonstrated by Avram and Xirouchakis (2011) that quantified the energy shares of the machine sub-systems strictly connected to the cutting process. Although the studies showed that the spindle energy consumption can be relevant both in high and low cutting speed machining, only few literature research works were focused on the component enhancement. For instance, Abele et al. (2011) outlined some potential ways for increasing the efficiency of spindle systems. Even Harris et al. (2015) dealt with spindle system energy consumption reduction but focusing on a too narrow application (ultra-high spindles). In fact, in this research an electric and a pneumatic spindle were compared from the electric power demands perspective.

Since the topic seems quite unexplored, in this paper it was decided to deeply analyze the energy saving opportunities of a novel spindle system conceptual design. More specifically, an innovative gear-less spindle solution suitable for multi-functional applications is studied from the energy consumption perspective. The development of such a solution was already indicated by Abele et al. (2010) as a future challenge in the development of a new generation of spindle systems. Moreover, the adoption of direct drive solutions is also promoted in ISO (2014) as an effective way for increasing the machine tool efficiency.

In the here presented research, the innovative spindle is compared with a classical spindle unit characterized by similar global performances but equipped with a gearbox-based module. The transmission makes the spindle adaptable to different applications (i.e. high torque, high speed cutting, drilling or threading). In the novel spindle solution, this adaptability is guaranteed by the electronic commutation of specifically designed stator winding circuits.

The elimination of the gearbox, together with the associated auxiliaries for

lubricating and cooling, makes the novel solution particularly interesting from the energy saving point of view. On the contrary, the electrical motor is forced working over a wider range of spindle-torque combinations in which the best electrical performances are probably not assured.

In this paper, a methodology for performing the energy assessment of the two alternative spindle solutions was devised. The energy analysis was carried out using a combined experimental-modeling approach.

The two spindle units, equipped with the relative auxiliaries, were first experimentally characterized on a test rig. Experimental test results were used to develop empirical models that were successively exploited for inferring about the energy savings linked to the proposed direct drive spindle solution. In order to accomplish this task, a realistic scenario of use for the spindle was considered. For making the study more general, a sensitive analysis changing the spindle working conditions used in the production batch emulation was carried out.

The paper is structure as follows. In section 2 a more detailed description of the analyzed spindle systems and the explanation of the adopted approach are provided. In section 3 the experimental campaign is properly discussed. In section 4 the obtained models are presented. In section 5, the results of model validation are presented. In section 6 the analyzes performed for estimating the potential energy savings are described. The main achieved results are properly discussed. Finally, in section 7 the conclusions are outlined.

Nomenclature

ΔE_S	energy saving due to the spindle
ΔE_{AUX_0}	achievable energy saving when the spindle is ready to operate
ΔE_{AUX}	achievable energy saving when the spindle is performing a proper cutting
ΔE_{S_K}	energy saving due to the spindle linked to the k-th machining operation
ΔE_{TOT}	overall energy saving
Δt_K	duration of the k-th machining operation
$\dot{\omega}_m$	spindle motor acceleration
η_S	spindle efficiency
η_{GS}	global spindle efficiency
$\hat{p_{mn}}$	generic losses model parameter estimation
ω_m	spindle motor velocity
τ	gearbox transmission ratio
c_{sF}	static friction coefficient
c_{vF}	viscous friction coefficient
E_{CE}	nominal cutting energy
E_{Mein}	overall machine energy
E_{Sein}	spindle energy
E_{SS-CE}	energy saving percentage with respect to the nominal cutting energy E_{CE}
E_{SS-M}	energy saving percentage referred to the overall absorbed machined energy E_{Mein}
E_{SS-S}	energy saving percentage referred to the absorbed spindle energy E_{Sein}
F	axes feed

f_s sampling frequency power measurements

i_{i_1}, i_{i_2}, i_{i_3} three-phase currents of subsystem i

i_{i_j} generic j^{th} current

J_m overall spindle inertia reduced to the motor side

$L_{S_{highspeed}}$ spindle losses high speed configuration

$L_{S_{lowspeed}}$ spindle losses low speed configuration

L_{SE} spindle electrical losses

L_{SFl} spindle friction losses of the *load*

L_{SFmgl} spindle friction losses of the group $motor + gearbox + load$ in the gearbox-based spindle

L_{SFmg} spindle friction losses of the group $motor + gearbox$ in the gearbox-based spindle

L_{SFml} spindle friction losses of the group $motor + load$ in direct drive spindle

L_{SFm} spindle friction losses of the *motor*

L_{SF} spindle friction losses

L_S spindle losses

n_K spindle speed during the k-th machining operation

p, k friction model identified parameters

P_i active power of the machine subsystem i

P_{AUXein_0}, m chiller model parameters

P_{AUXein} auxiliary equipment power consumption

P_{cutt} cutting power

P_{GCein} electrical power absorbed by the chiller of the gearbox

P_{Gein} spindle global power consumption

P_{Mein} overall machine power

p_{mn} generic losses model parameter

P_{Mout} requested mechanical power

P_{Pein} pump electrical power

P_{SCein} electrical power absorbed by the chiller of the motor

P_{Sein} spindle electrical power

$R_{sq_{adj}}$ coefficient of determination of the regression

T spindle torque

t time

T_0 ready to operate state duration

T_K requested average spindle torque for the k-th machining operation

T_P analyzed production time period

$t_{2_j} - t_{1_j}$ duration of the j^{th} long run test(type B)

T_F friction torque

v_{i_1}, v_{i_2}, v_{i_3} three-phase voltages of subsystem i

2. Materials and methods

The relevance of the spindle system is demonstrated by numerous researches that were developed over the years for increasing performance and reliability of such a relevant machine tool component. In a key note paper, Abele et al. (2010) summarized the principal achieved results and outlined the main challenges in spindle future research:

- development of spindle technology for high torque and high speed multi-functional applications
- energy consumption reduction focusing also on the peripheral equipment for drive, bearings, gearbox and on cooling system
- development of gear-less spindle solutions for high torque demanding applications (i.e. hard to cut materials like titanium alloys).

The listed challenges are also pulled by the market.

In the framework of the founded research project (EROD Energy Reduction Oriented Design), a spindle solution that fulfils the above reported specifications was developed in collaboration with a machine tool builder (Jobs) and a spindle manufacturer (HSD). The here presented research mainly focuses on the study of the energy saving opportunities linked the developed solution.

2.1. Spindle systems description

Since machine tools usually need to perform several machining operations on the same work-part, the spindle system has to be adequately designed for assuring the requested flexibility and the desired performances over such a wide range of working conditions. In modern machines, these challenging requirements are satisfied with consolidated design solutions. In most of the machine tools conceived for multiple applications, the spindle motor is connected to the cutting tool through a shiftable gearbox. In addition, sometimes a mechanical transmission can also be found. When high torque machining operations need to be carried out, the gearbox, reducing the rotating speed of the electrical motor, provides the desired torque amplification. On the contrary, when high spindle speed operations need to be executed, the gearbox directly couples the electrical motor with the spindle shaft. This spindle solution is typically equipped with two chiller units and a hydraulic pump. The main chiller cools the electrical motor removing the losses related heat (i.e. bearing losses, viscous shear of air and electric motor losses). The pump assures a inlet flow of oil in the gearbox for lubrication and cooling purposes. The second chiller keeps the temperature of the motor oil within a suitable range.

The schematic representation of the above described solution, for the studied Jobs machine ($Jomax265$), is reported in Figure 1, left side. Specifically, the spindle is equipped with an asynchronous AC Kessler motor and a Redex shiftable gearbox (transmission ratio $\tau = 1 : 5$). The motor and the gearbox chiller units (respectively KRA70J and KRO60J) are produced by Kelvin.

Although this spindle system solution is widespread in modern machines, it exhibits some weak points. Indeed, the described solution is highly energy demanding. This is due to the auxiliary equipment (chillers and pump) requested for cooling the system. In addition, the losses associated to the gearbox contribute making this solution not particularly efficient. In order to overcome this issue, a novel gear-less spindle system solution was developed in the EROD project. The new devised spindle system configuration is rather simplified: the gearbox, the oil pump and the gearbox chiller were eliminated (Figure 1, right

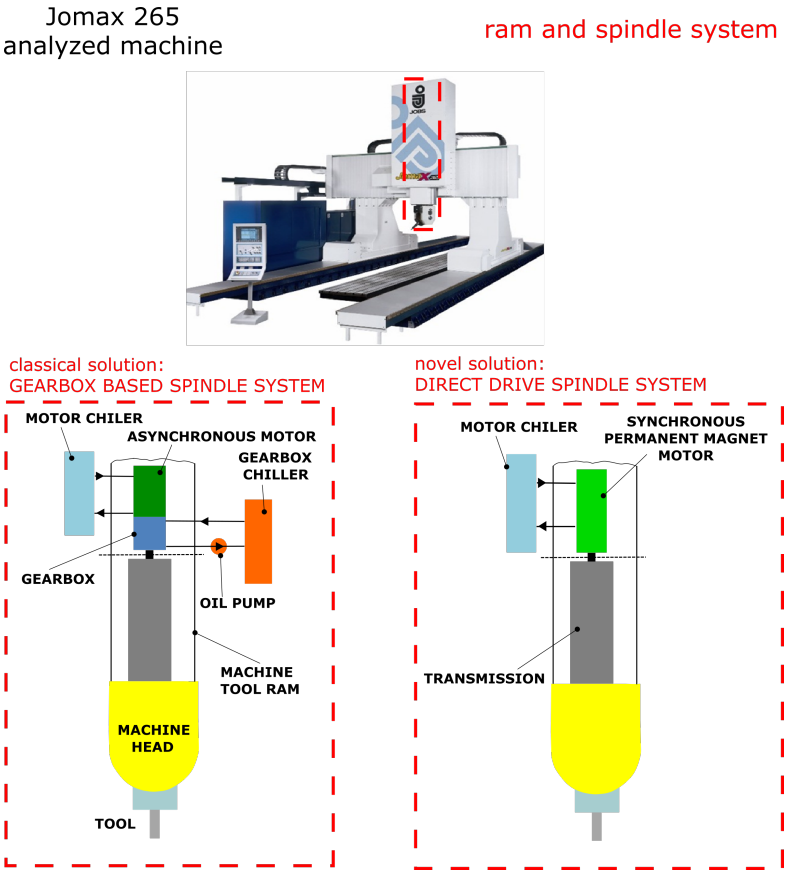

Figure 1: analyzed machine and spindle solutions comparison

side). The spindle is equipped with a HSD permanent magnet synchronous motor PMSM that assures, exploiting two different specifically designed stator windings, comparable performances in terms of the speed-torque characteristic curve.

2.2. Description of the adopted approach

Although a rough estimation of the energy savings linked to the simplifications introduced to the auxiliary equipment can be easily envisaged, a comprehensive energy assessment of the two alternative spindle solutions is far from being an easy task and it requires a structured approach. In fact, several trade-offs need to be investigated. For example, the novel spindle solution, being based on a PMSM motor that is forced working over an extremely wide spindle speed range, could hardly achieve the motor efficiency assured by the AC asynchronous solution that exploits the amplification/reduction properties of

the gearbox. Conversely, the gearbox is responsible for additional losses. Moreover, since the power absorbed by the chiller units strictly depends on the motor losses, as demonstrated by (Calvanese et al., 2013), a different chiller behaviour is expected in the compared spindle installations.

In order to accomplish this task, a specific analysis approach was conceived, Figure 2. It is based on the development of reliable energy models for both

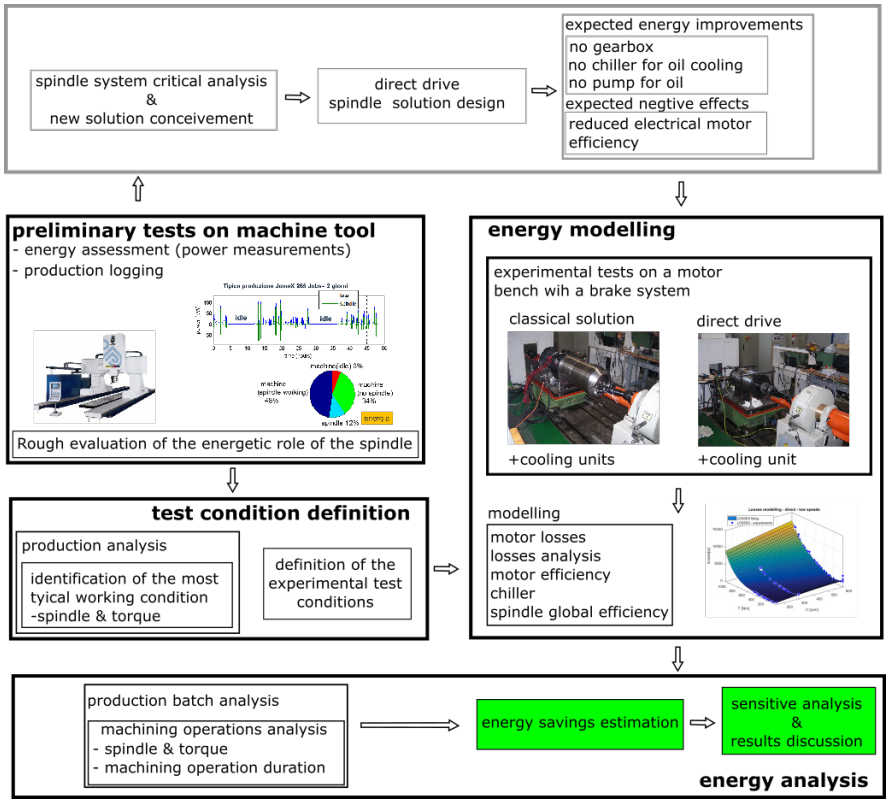

Figure 2: Approach used for the energy saving analysis - paper content (bold rectangles)

the spindle systems. Even the auxiliaries were considered in the model. As suggested by Balogun and Mativenga (2013), an empirical approach was used in different phases of the model development (Section 4): motor losses modeling, auxiliary equipment modeling, spindle efficiency modeling and spindle system global efficiency modeling.

The choice of adopting an empirical approach also for modeling the electrical motor losses was supported by a scientific literature analysis. In fact, although several studies on the motor losses modeling, both using analytical (i.e. Rahman and Zhou (1996)) or finite element FE approaches (i.e. Sizov et al. (2012)), have been done over the years, the empirical approach is still a largely diffused methodology for the electrical motors characterization. Moreover, the empirical

approach allows taking into account the unknown losses such as the stray losses (Jimoh et al. (1985)). Since the the necessity of considering the heat generated in the the spindle and the role of the auxiliary equipment (chiller units and gearbox), the empirical approach seemed the sole suitable methodology for obtaining a reliable energy model of the overall spindle system. This is confirmed by the fact that the estimation of the heat generated through model is a challenging task and requires several experiments to identify the unknown model parameters, Bossmanns and Tu (1999).

For identifying the described models, both the spindles were experimentally tested on a specific motor bench equipped with brakes (Subsection 3.2). This allowed characterizing the spindles in different realistic cutting conditions, just reproduced setting the spindle speed and the breaking torque (cutting torque) at the desired values. Further details on the adopted experimental procedure are reported in Section 3. Suitable test conditions ("test condition definition") for the models development were defined (Subsection 3.1.2) analyzing the data acquired during two working (preliminary tests). These tests (Subsection 3.1) were also useful for performing a first rough machine tool energy assessment that put into evidence the role of the spindle in the overall machine tool energy consumption (Subsection 3.1.1). The developed models (Section 4) were used for performing a meaningful energy assessment ("energy analysis") and a quantification of the achievable energy savings (Section 6). This was done simulating the execution of a set of machining operations that belong to a real production batch. For sake of generality, sensitive analyses considering different machine task combinations were also carried out.

3. Spindle system experimental characterization

3.1. Preliminary tests on the machine during production

3.1.1. Power measurements and machine tool energy assessment

Some power measurements were carried out on the analyzed machine in order to obtain a preliminary energy characterization. In accordance with the guidelines under definition in (ISO, 2016), the energy assessment was done in the following machine configurations:

- machine in the "ready to operate" state
- machine during the execution of some production batches

For this purpose, the machine was equipped with a specifically designed power meter able to measure and storage power data of multiple electric loads. The following machine sub-systems were characterized: electrical cabinet, numerical controller NC, human machine interface HMI, machine drives, hydraulic unit, pumps and chillers. If a direct power measurement on a component was not possible, the absorbed power was estimated through differential power measurements. The active power of each considered machine subsystem $P_i(t)$ was computed considering $P_i(t) = i_{i_1}(t)v_{i_1}(t)+i_{i_2}(t)v_{i_2}(t)+i_{i_3}(t)v_{i_3}(t)$, where $v_{i_1}(t)$,

$v_{i_2}(t)$, $v_{i_3}(t)$ are the three-phases voltages and ($i_{i_1}(t)$, $i_{i_2}(t)$, $i_{i_3}(t)$) are the corresponding absorbed currents. All the electrical quantities were acquired at a high sampling rate, $f_s = 30\,\text{kHz}$. The generic current $i_{i_j}(t)$ was measured using a LEM ring based on the Hall's principle.

The power absorbed by the machine and its main subcomponents in the "ready to operate" state are mapped in Figure 3. The machine drives together

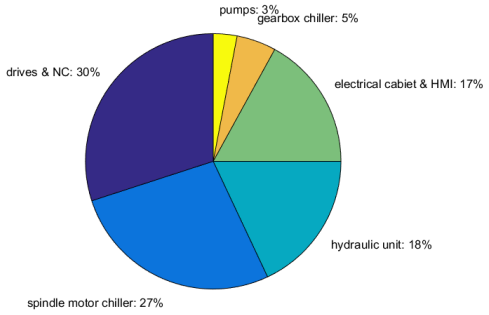

Figure 3: Ready to operate machine - power consumption distribution

with the NC unit absorb up to 30% (2.3 kW) of the whole machine global power (7.78 kW). Also the hydraulic unit plays a quite relevant role in terms of absorbed energy, 1.4 kW (18%). It is worth of noting that the spindle auxiliary equipment (motor chiller (2.12 kW) , oil pump (0.26 kW) and gearbox chiller (0.4 kW)) accounted for 35% of the overall energy.

For what concerns the energy assessment of the "shift regime" (according to ISO (2016) is a set of a representative tasks typically performed by the machine) it was decided to monitor mainly the global machine power and the spindle power. In this specific case, the powers were acquired for 48 h, while the machine was processing real pieces. The production batches analysis brought to the conclusion that the machine was in the "idle" state for 34% of the analyzed time period T_P, the spindle was active for 35% of T_P and for the rest of the time the machine was active but without performing any machining operations. The map of the used energy is reported in Figure 4. This analysis was done in order to have an idea of the spindle contribution on the total absorbed energy. The overall machine energy E_{Mein} was computed integrating the measured machine power $P_{Mein}(t)$ over T_P, Eq. 1. It can be observed that the machine consumed about 6% of the overall energy E_{Mein} during the idle state, 34% when the spindle was not working and 48% when the the spindle was rotating.

$$E_{Mein} = \int_0^{T_P} P_{Mein}(t)\,dt \tag{1}$$

The spindle energy E_{Sein} (computed integrating the measured spindle power $P_{Sein}(t)$, Eq. 2) accounted for the 12% (178.8 MJ) of the total energy (1.49 GJ).

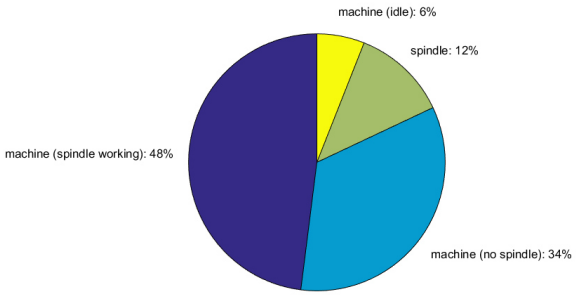

Figure 4: Production analysis - energy distribution

$$E_{Sein} = \int_0^{T_P} P_{Sein}(t)\, dt \tag{2}$$

Although the spindle contribution E_{Sein} (the sole linked to the electrical motor) was not the predominant one, it can be noted that the machine consumed a lot of energy (about 48%) when the spindle was active. This means that the spindle auxiliary equipment (chillers and the oil pump) played an important role from the energy consumption perspective. This can be appreciated also looking at Figure 5, where both the spindle power and the power of the rest of the machine are reported for a portion of the analyzed production. It is clearly visible that when the spindle was working, even the rest of the machine was absorbing more power (+46%) with respect to the power absorbed when the spindle was not machining. This confirmed the importance of including the spindle related equipment in the energy analysis. This means that the power consumption of some machine tool subsystems (i.e. auxiliary equipment) is strongly related to the spindle losses. This relationship was not typically considered in almost all the papers on machine tool or spindle energy modeling.

3.1.2. Production analysis

A production logging system based on OPC server was set to monitor the machine during real production. In particular, the information about the tool code, the axes feed F, the spindle speed n and the spindle torque T were gathered. analyzing the acquired data, it was observed that the majority of the performed milling operations (mainly on steel and cast iron) were characterized by a spindle speed n that ranged from 180 rpm to 510 rpm and a spindle torque T that is within the 10-500 Nm interval. These machining operations were executed with the spindle system set in the low speed-high torque configuration. For what concerns the machining operations carried out with the spindle in the high velocity configuration (i.e. drilling, threading), it was observed that the spindle speed n was set within the 2,700-3,200 rpm interval while the requested

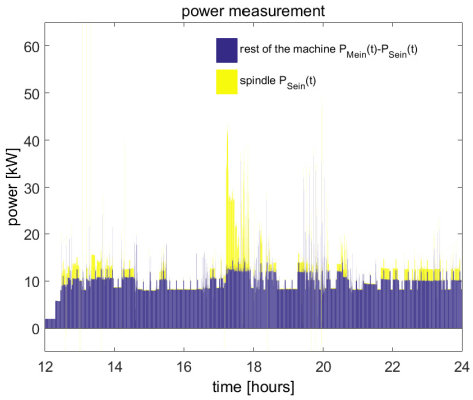

Figure 5: Power measurement during the execution of a production batch

torque T was extremely low (approximately negligible). This preparatory analysis was helpful for defining the experimental conditions to be reproduced on the spindle bench, subsection 3.2.3.

3.2. Spindle system empirical energy characterization

In this paper section a detailed description of the experimental procedure adopted for the spindle system energy characterization is provided. Data acquired during the experiments were used for the energy models development, section 4.

3.2.1. Energy model description

Before proceeding with the experimental procedure explanation, a general description of the adopted modeling approach is useful for a better comprehension of some performed choices. Figure 6 accomplishes this task. Indeed, it shows a conceptual representation of the analyzed spindles with the system boundary definition and the considered energy flows. Moreover, the scheme shows how each spindle solution was experimentally characterized on the test bench.

The conceived model (Eq. 3) links the spindle global power consumption P_{Gein} to the requested mechanical power P_{Mout} that in this case stands for the requested cutting power P_{cutt}. The following relationship can be written defining the spindle speed n and torque T, $P_{Mout}(n,T) \equiv P_{cutt} = T \cdot n$.

$$P_{Gein} = f\big(P_{Mout}(\Omega, T)\big) \tag{3}$$

Using the model reported in Eq. 3 it would be possible to estimate the spindle power consumption for any cutting operation described by T and n.

As can be observed in Figure 6, P_{Gein} is the summation of the following contributions:

$$P_{Gein}(n,T) = P_{AUXein}(n,T) + P_{Sein}(n,T) \tag{4}$$

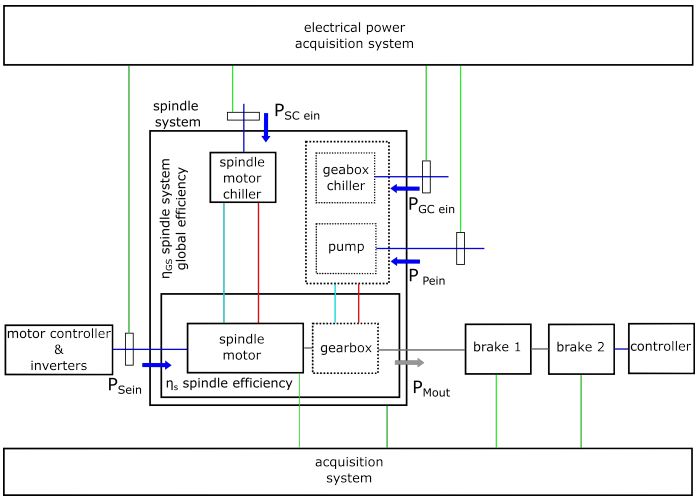

Figure 6: Schematic representation of the spindle on the bench - system boundaries and energy flows definition

where P_{Sein} is the electrical power absorbed by the spindle motor while P_{AUXein} is the power consumption linked to the auxiliary equipment that depends on the analyzed spindle system configuration. For instance, if the gearbox-based solution is considered, P_{AUXein} can be computed through Eq. 5.

$$P_{AUXein}(n,T) = P_{SCein}(n,T) + P_{GCein}(n,T) + P_{Pein}(n,T) \tag{5}$$

where where P_{SCein} is the electrical power absorbed by the motor chiller, P_{GCein} is the electrical power absorbed by the gearbox chiller and P_{Pein} is the electrical power absorbed by the pump.

In terms of efficiency, according to Boglietli et al. (2003), the spindle efficiency can be therefore computed with Eq. 6

$$\eta_S(n,T) = \frac{P_{Mout}(n,T)}{P_{Sein}(n,T)} \tag{6}$$

Generalizing the concept to the overall spindle system, the global spindle efficiency η_{GS} can be computed through Eq. 7:

$$\eta_{GS}(n,T) = \frac{P_{Mout}(n,T)}{P_{Gein}(n,T)} \tag{7}$$

When a generic machining operation, performed at n, requires the cutting torque T, the overall spindle global power consumption can be estimated through Eq. 8

$$P_{Gein} = \frac{T \cdot n}{\eta_{GS}(n,T)} \tag{8}$$

The above equation cannot be used when the cutting power $P_{Mout} = 0$. In such a case, the spindle system global consumption needs to be calculated through Eq. 4.

The key point for developing the described model is the characterization of the overall spindle losses L_S as a function of n and T, Eq. 9:

$$L_S(n,T) = \big(P_{Sein}(n,T) - P_{Mout}(n,T)\big) \tag{9}$$

Focusing on the losses L_S, it was assumed that two main contributions are dominant, Eq. 10. One linked to friction $L_{SF}(n)$ that is affected mainly by the spindle speed n and another one associated to electric losses $L_{SE}(n,T)$. More details on the adopted friction model are provided in Section 4.

$$L_S(n,T) = L_{SF}(n) + L_{SE}(n,T) \tag{10}$$

Eq. 4, Eq. 6 and Eq. 7 can be written in another way putting into evidence the losses L_S:

$$P_{Gein}(n,T) = P_{Mout}(n,T) + L_S(n,T) + P_{AUXein}(n,T) \tag{11}$$

$$\eta_S(n,T) = \frac{P_{Mout}(n,T)}{\big(P_{Mout}(n,T) + L_S(n,T)\big)} \tag{12}$$

$$\eta_{GS}(n,T) = \frac{P_{Mout}(n,T)}{\big(P_{Mout}(n,T) + L_S(n,T) + P_{AUXein}(n,T)\big)} \tag{13}$$

For being able to estimate η_{GS}, the auxiliary equipment power model $P_{AUXein}(n,T) = f\big(L_S(n,T)\big)$ is therefore necessary. Such a model puts into relationships the overall electrical power absorbed by the auxiliaries P_{AUXein} and the spindle losses L_S as defined in Eq. 9. In fact, the availability of $P_{AUXein}(n,T)$ and $L_S(n,T)$ allows computing P_{Gein}, η_S, η_{GS}.

It is worth of noting that both the losses $L_S(n,T)$ and the auxiliaries $P_{AUXein}(n,T) = f\big(L_S(n,T)\big)$ models were empirically determined.

For this purpose, as shown in Figure 6, experimental tests were performed on the bench changing the spindle loading conditions (n – T) and monitoring the P_{GCein}, P_{SCein}, P_{Pein} and P_{Sein} powers.

Moreover, in order to analyze the mechanisms that rule the spindle losses L_S (i.e. friction or electrical losses), some specific tests were carried out. More details can be found in Section 3.2.2 and Section 3.2.3

3.2.2. Experimental set-up description

The test bench used for the characterization of the spindle systems was depicted in Figure 7. It is composed of a spindle system bed that holds the spindle motor, two brakes connected in series with the control unit (Apicom VIBRU), a joint that mechanically connects the spindle shaft to the brakes and a module containing the spindle motor controller and the related drives (Siemens Simodrive 611). The test bench was also equipped with sensors and acquisition systems.

More specifically, the following quantities were measured during the tests:

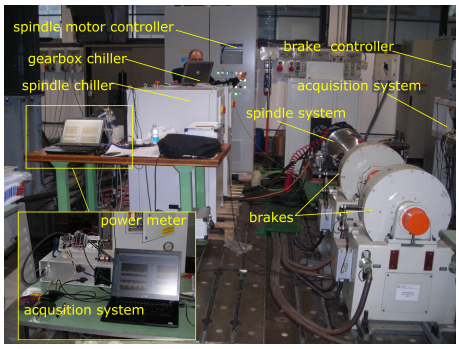

Figure 7: Test bench and instrumentation set-up

- overall torque T provided by the brakes (through Revere Transducers 363D3)
- spindle speed n through an encoder.
- currents and voltages of all the analyzed sub-units for the power computation of: P_{SCein}, P_{GCein}, P_{Pein} and P_{Sein}. The power computation of each unit was performed as described for the whole machine in the preliminary tests.
- temperatures (i.e. spindle and chiller temperatures). These quantities were acquired in order to monitor the thermal load of the spindle (especially spindle bearings) and of the chillers.

3.2.3. Test description

For both the spindle system configurations two different test sessions were carried out.

- test A. According to Eq. 12, some tests were performed for the characterization of $\eta_S(n, T)$. For each selected spindle speed n, the overall brake load T (emulation of the cutting torque) was progressively increased up to the desired value that mainly depends on the technological requirements defined in subsection 3.1.2. Both P_{Mout} and P_{Sein} were measured during the tests. Spindle losses and consequently the η_S were computed respectively with Eq. 9 and Eq. 12. Such tests were repeated at different speeds both in the high torque and high velocity spindle configurations.

  In Table 1 and Table 2 the experimental conditions used for the tests are reported.

- test B. This session was specifically conceived for the identification of the $P_{AUXein}(n, T) = f\big(L_S(n, T)\big)$ relationship. The tests were carried out following the approach suggested in (Albertelli et al., 2016) where a linear

Test Type	Configuration	n [rpm]	T [Nm]
Type A	high torque	150	0; 35; 83; 110; 164; 224; 260; 304; 349; 407; 470
Type A	high torque	300	0; 56; 100; 148; 207; 282; 313; 409; 458; 511; 570; 611
Type A	high torque	600	0; 5; 10; 14; 25; 31; 57; 74; 99; 127; 152; 205; 255; 303; 344; 394; 412; 516; 573; 614; 666
Type A	high speed	2,500	0; 3; 5; 9; 16; 32; 39; 47; 56; 64; 75; 101; 125; 136; 152
Type A	high speed	3,000	0; 4; 18; 21; 38; 59; 80; 84; 100; 111; 121; 132; 144
Type A	high torque	3,500	0; 5; 11; 13; 21; 40; 45; 50; 56; 68; 91; 100; 110; 120
Type B	high torque	300	800
Type B	high torque	600	210
Type B	high speed	1,500	160

Table 1: Experimental test conditions for the gearbox-based spindle solution

model was proposed for the machine tool chiller units, Eq. 14.

$$P_{AUXein}(n,T) = P_{AUXein_0} + m \cdot L_S(n,T) \tag{14}$$

The model parameters (P_{AUXein_0} and m) were identified through an experimental data regression procedure. More specifically, some tests were performed changing the loading conditions. For each test case, both the losses L_s and the P_{AUXein} were evaluated. In order to assure the achievement of the thermal stability, long run tests were carried out. For this purpose some temperatures were measured during the tests. Since both $P_{AUXein} = f(t)$ and $L_S = f(t)$ are time dependent (due to the chiller control strategy), the average values $\overline{P_{AUXein}}$ and $\overline{L_s}$ were computed before developing the energy model. For instance, focusing on the generic test performed with the T_j-n_j combination, it was done using the following relationships.

$$\overline{P_{AUXein}}(n_j,T_j) = \frac{1}{t_{2_j} - t_{1_j}} \int_{t_{1_j}}^{t_{2_j}} P_{AUXein}(n_j,T_j,t)\,dt \tag{15}$$

$$\overline{L_S}(n_j,T_j) = \frac{1}{t_{2_j} - t_{1_j}} \int_{t_{1_j}}^{t_{2_j}} L_S(n_j,T_j,t)\,dt \tag{16}$$

where $t_{2_j} - t_{1_j}$ is the duration of the j^{th} long run test. The auxiliary equipment model was developed exploiting at least three different working conditions $L_S(n,T)$, see Table 1 and Table 2.

Test Type	Configuration	n [rpm]	T [Nm]
Type A	high torque	150	0; 6; 75; 100; 162; 200; 246; 298; 354; 401; 445; 469
Type A	high torque	300	0; 56; 100; 157; 198; 253; 315; 354; 397; 458; 498; 600; 633; 692
Type A	high torque	600	0; 50; 92; 102; 129; 203; 277; 302; 349; 398; 453; 498; 532; 599; 691
Type A	high speed	2,500	0; 1; 29; 48; 54; 94; 103; 149; 173; 200; 211; 221; 242
Type A	high speed	3,000	0; 2; 43; 49; 64; 90; 98; 125; 147; 149; 170; 189
Type A	high torque	3,500	0; 3; 21; 43; 50; 99; 114; 147; 158
Type B	high torque	300	800
Type B	high torque	600	800
Type B	high speed	1,500	210
Type B	high speed	3,000	170

Table 2: Experimental test conditions for the direct drive spindle solution

- test C. According to Eq. 10, a specific experimental procedure was conceived for the spindle friction losses L_{SF} characterization. For this purpose, coast tests were carried out for both the spindle systems. The test consists in putting into rotation the spindle system at a certain rotation speed, unplug the motor from the drive and wait until the spindle naturally stops due to friction. Since the motor was not connected to the drive, the adopted procedure assured to identify the sole contribution due to friction L_SF. A similar methodology was also used in (Bossmanns and Tu, 2001).

  The relationship that describes the dynamic equilibrium of the system during the coast test is reported in Eq. 17. J_m $[kg \cdot m^2]$ is the overall spindle inertia reduced to the motor side, $\dot{\omega}_m$ $[rad/s^2]$ the motor acceleration and T_F $[Nm]$ the overall present friction torque referred to the motor.

$$J_m \cdot \dot{\omega}_m(t) + T_F(\omega_m) = 0 \tag{17}$$

  Since the overall inertia J_m can be easily identified using a specific procedure available on the motor drive, $\omega_m(t)$ is measured during the test and subsequently derived, the friction torque, at different speeds, can be computed using Eq. 17. Consequently, the friction power losses $L_{SF}(n)$ as a function of the spindle speed n can therefore be estimated:

$$L_{SF}(n) = T_F(n) \cdot \frac{60 \cdot n}{2\pi \cdot \tau} \tag{18}$$

  Repeating the coast test with different spindle configurations (i.e. for the gearbox-based spindle system), it was also possible to characterize the friction contribution associated to the motor shaft (mainly due to the

friction of bearings and the viscous shear of air), associated to the gearbox (for both the available gearbox shifts) and to the load (i.e. the friction introduced by the brake for the tests performed on the test-bench).

The same characterization approach was used also for the direct drive spindle solution. In Eq. 18, depending on the analyzed configuration, the transmission ratio was set at $\tau = 1$ (i.e. for direct drive spindle system or for the gearbox-based spindle when used at high speeds) and at $\tau = 1/5$ when the gearbox-based spindle is used in the low speed range.

4. Spindle system energy modeling

4.1. Spindle losses modeling

A multiple linear regression approach (Montgomery, 2001) was used for developing empirical models.

The spindle losses models $L_S(n, T)$ were developed first. Polynomial functions were used for fitting the experimental data, Figure 8. A specific model

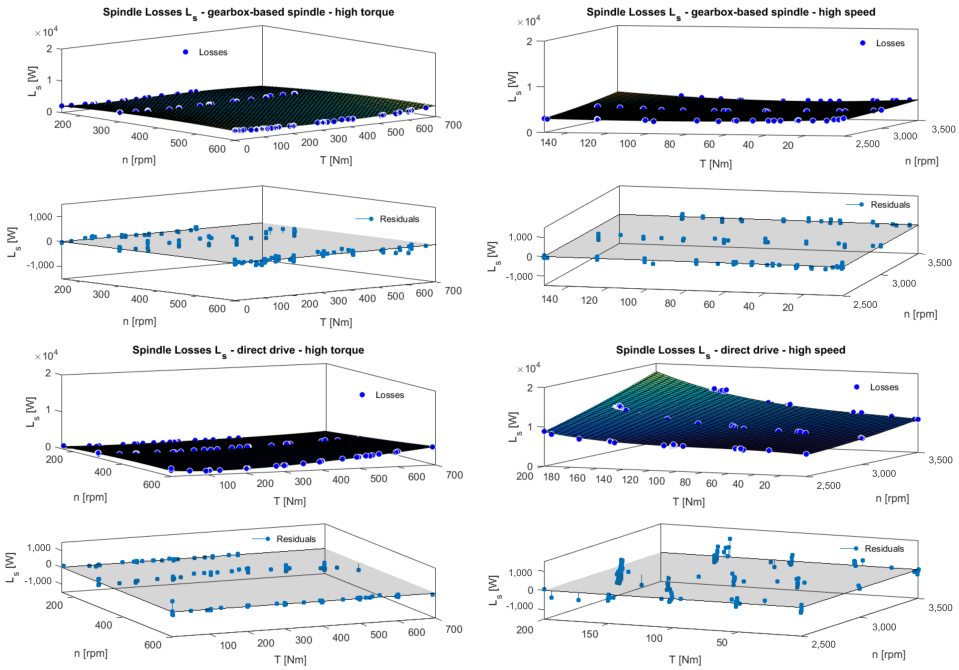

Figure 8: Spindle losses regression - spindle solutions comparison

was developed according to the analyzed spindle system configuration (low/high speed). For instance, a 2^{nd}-order function in the variable n and a 4^{th}-order function in the variable T (Eq. 19) was used for modeling the losses when the spindle is in the low speed configuration. For the high spindle speed range, it was found

that functions of the 2^{nd}-order in the variable n and a 3^{rd}-order function in the variable T (Eq. 20) fit quite well the experimental data of both the spindles. Referring to Eq. 19 and Eq. 20, p_{mn} are the regression coefficients that were estimated ($\hat{p}_{mn}$) through a least square minimization. ϵ is the error term in the models. For all the regressions quite high coefficients of determination ($R_{sq_{adj}} > 0.98$) were found.

$$\begin{aligned} L_{S_{lowspeed}}(n,T) = {} & p_{00} + p_{10}\cdot n + p_{01}\cdot T + \\ & p_{20}\cdot n^2 + p_{11}\cdot n\cdot T + p_{02}\cdot T^2 + \\ & p_{21}\cdot n^2\cdot T + p_{12}\cdot n\cdot T^2 + p_{03}\cdot T^3 + \\ & p_{22}\cdot n^2\cdot T^2 + p_{13}\cdot n\cdot T^3 + p_{04}\cdot T^4 + \epsilon \end{aligned} \tag{19}$$

$$\begin{aligned} L_{S_{highspeed}}(n,T) = {} & p_{00} + p_{10}\cdot n + p_{01}\cdot T + \\ & p_{20}\cdot n^2 + p_{11}\cdot n\cdot T + p_{02}\cdot T^2 + \\ & p_{21}\cdot n^2\cdot T + p_{12}\cdot n\cdot T^2 + p_{03}\cdot T^3 + \epsilon \end{aligned} \tag{20}$$

In Figure 8, the residuals plots are also reported for each developed model. The identified parameters are reported below:

- gearbox-based spindle (high torque configuration): $p_{00} = 2,329$, $p_{10} = 123.5$, $p_{01} = 471.1$, $p_{11} = 86.62$, $p_{20} = -172.4$, $p_{02} = 546.1$, $p_{21} = -172.6$, $p_{12} = 298$, $p_{03} = 196.1$, $p_{22} = -176.7$, $p_{13} = 184.1$, $p_{04} = 123.9$ where n is normalized by mean $483.3\,rpm$ and standard deviation $183.6\,rpm$ and similarly T is normalized by mean $468.8\,Nm$ and standard deviation $269.6\,Nm$

- direct-drive spindle system (high torque configuration): $p_{00} = 2,456$, $p_{10} = 931.3$, $p_{01} = 1,933$, $p_{11} = 536.6$, $p_{20} = 71.67$, $p_{02} = 800.2$, $p_{21} = -44.38$, $p_{12} = -11.15$, $p_{03} = 327.7$, $p_{22} = -54.75$, $p_{13} = -57.44$, $p_{04} = 107.7$ where n is normalized by mean $356.1\,rpm$ and standard deviation $142.3\,rpm$ and similarly T is normalized by mean $628.7\,Nm$ and standard deviation $265.3\,Nm$

- gearbox-based spindle (high speed configuration): $p_{00} = 3,083$, $p_{10} = 278.4$, $p_{01} = -188.5$, $p_{11} = 110.7$, $p_{20} = 110$, $p_{02} = 287.9$, $p_{21} = 32.89$, $p_{12} = 100.6$, $p_{03} = -20.21$ where n is normalized by mean $2821\,rpm$ and standard deviation $402.3\,rpm$ and similarly T is normalized by mean $63.2\,Nm$ and standard deviation $49.08\,Nm$

- direct-drive spindle (high speed configuration): $p_{00} = 9,340$, $p_{10} = 2,306$, $p_{01} = 2,652$, $p_{11} = 1,133$, $p_{20} = 243.9$, $p_{02} = 1,260$, $p_{21} = 5.972$, $p_{12} = 2,42$, $p_{03} = 268.1$ where n is normalized by mean $2,922\,rpm$ and standard deviation $375.6\,rpm$ and similarly T is normalized by mean $153.3\,Nm$ and standard deviation $60.83\,Nm$

4.2. Spindle losses analysis

Regarding the losses analysis, as anticipated in the previous section, specific tests were executed to identify the power losses due to friction. The model reported in Eq.17 was further developed assuming that the friction torque T_F is twofold, Eq. 21.

$$J_m \cdot \dot{\omega}_m(t) + c_{vF} \cdot \omega_m(t) + c_{sF} = 0 \tag{21}$$

Where c_{vF} is the viscous friction coefficient and c_{sF} the static friction coefficient. The parameters of the model can be identified through a regression procedure. More specifically, the experimentally measured motor speed $\omega_m(t)$ was fitted with the solution (Eq. 23) of the first order differential equation that describes the free spindle deceleration (Eq. 22).

$$\begin{cases} \dot{\omega}_m(t) + \frac{c_{vF}}{J_m} \cdot \omega_m(t) = -\frac{c_{sF}}{J_m} \\ \omega_m(0) = \omega_{m0} \end{cases} \tag{22}$$

Where ω_{m0} represents the initial condition.

$$\omega_m(t) = \omega_{m0} \cdot e^{-\frac{c_{vF}}{J_m} \cdot t} - \frac{c_{sF}}{c_{vF}} + \frac{c_{sF}}{c_{vF}} \cdot e^{-\frac{c_{vF}}{J_m} \cdot t} \tag{23}$$

Eq. 23 was rewritten (Eq. 24) just after having defined the following quantities: $p = -c_{vF}/J_m$ and $k = -c_{sF}/c_{vF}$.

$$\omega_m(t) = \omega_{m0} \cdot e^{-p \cdot t} + k - k \cdot e^{-p \cdot t} \tag{24}$$

p and k were estimated through the regression procedure. The friction model parameters c_{sF} and c_{vF} were further computed.

For sake of generality, the friction characterization procedure is here demonstrated for the gearbox-based spindle. Indeed, in such case the identification of the friction contribution due to the gearbox was also necessary. Referring to Fig. 9, the deceleration curves $\omega_m(t)$ of the spindle in three different configurations are reported. The motor with the coupled gearbox ($motor + gearbox$) was the first tested system. The gearbox was set in the high shift configuration. The test was also repeated mechanically connecting the load to the motor-gearbox group ($motor$+$gearbox$+$load$). The friction contribution due to the brake ($load$) resulted from the subtraction of the previously identified friction parameters. The third test was executed with the gearbox in the low speed configuration. The identified friction parameters are reported in Table 3. Similar experiments were also carried out with the sole electrical motor in order to characterize the friction contribution L_{SFm} due to the bearings and due to the viscous shear of air, Bossmanns and Tu (2001).

The friction parameters estimation relies on (Eq. 23 and Eq. 24) a former system inertia J_m identification. It was carried out through a specific tool available on the Siemens drive. The identified moments of inertia are reported in Table 4. Just as an example, the regression of one of the deceleration curves is reported

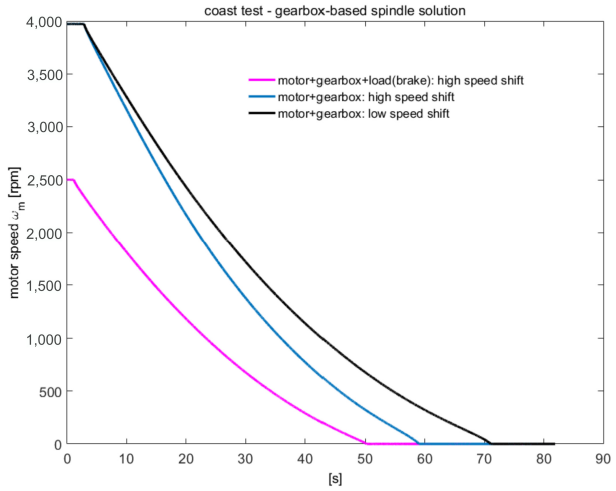

Figure 9: Coast test - gearbox-based spindle

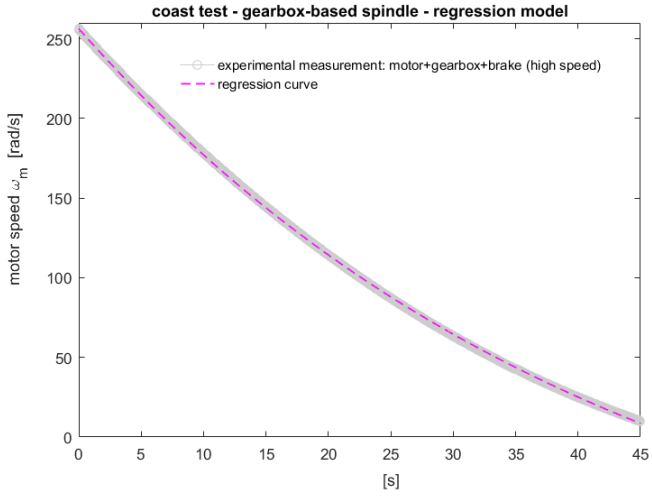

Figure 10: Coast test - example of regression curve

test configuration	$c_{vF}\,[Nm/(rad/s)]$	$c_{sF}\,[Nm]$
$motor + gearbox + load$ (high speed shift)	0.0144	1.8
$motor + gearbox$ (high speed shift)	0.0074	1.1324
$motor + gearbox$ (low speed shift)	0.0054	0.7924
$load$	0.007	0.6696

Table 3: Identified friction coefficients

test configuration	$J_m\,[kg \cdot m^2]$
$motor + gearbox + load$ (high speed shift)	0.618
$motor + gearbox$ (high speed shift)	0.312
$motor + gearbox$ (low speed shift)	0.27

Table 4: Identified inertia

in Fig. 10. The model shows a good agreement with the experimental measurements. For all the analyzed cases, quite high coefficients of determination ($R_{sq_{adj}} > 0.99$) were found. Moreover, the comparison between the measured friction power (Eq. 17) and the friction power computed using the implemented model (Eq. 21) is reported in Fig. 11. The good matching between the curves shows that even a quite simple model can be used to predict the friction losses in a spindle system. Eq. 10 can therefore be rewritten putting into evidence all

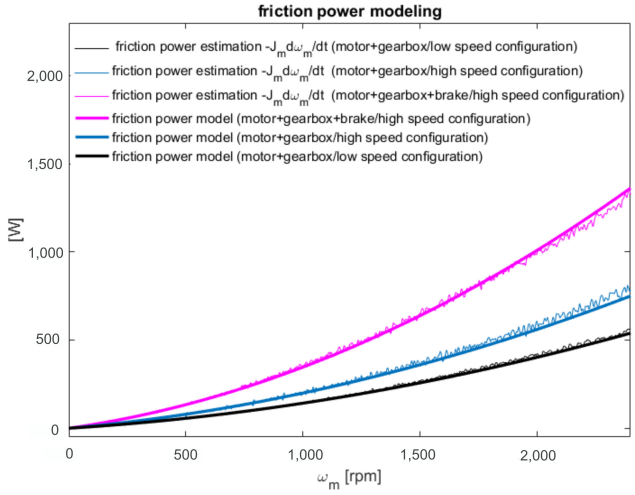

Figure 11: Friction power comparison - estimated through measurements Vs estimated through model

the identified losses contributions. For what concerns the direct drive spindle

solution, Eq. 10 becomes Eq. 25

$$\begin{aligned} L_S(n,T) = L_{SE}(n,T) + L_{SF}(n) = L_{SE}(n,T) + L_{SFml}(n) = \\ = L_{SE}(n,T) + L_{SFm}(n) + L_{SFl}(n) \end{aligned} \tag{25}$$

where the friction losses $L_{SF} \equiv L_{SFml}$ accounts for the contribution of the *motor* L_{SFm} and the contribution of the *load* L_{SFl}. L_{SFm} can be neglected if compared to other terms, especially when the direct drive spindle is rotating at low speeds. For the gearbox-based spindle system, the following equation can be written:

$$\begin{aligned} L_S(n,T) = L_{SE}(n,T) + L_{SF}(n) = L_{SE}(n,T) + L_{SFmgl}(n) = \\ = L_{SE}(n,T) + L_{SFmg}(n) + L_{SFl}(n) \end{aligned} \tag{26}$$

where the friction losses $L_{SF} \equiv L_{SFmgl}$ accounts for the *motor+gearbox* friction losses L_{SFmg} and for the *load* L_{SFl} contribution. It was found that L_{SFmg} is mainly due to the the contribution linked the gearbox rather than the one connected to the *motor* L_{SFm}. When the gearbox-based spindle rotates at low speed, L_{SFm} is higher than the corresponding one in the direct drive. This is linked to the fact that the motor, due to the role of the gearbox, is rotating at higher speeds if compared to the load. On the contrary, the friction losses L_{SFm} are similar in both the spindle systems for the high-speed rotating speeds. Fig. 12 and Fig. 13 underline the main losses contributions defined in Eq. 25 and Eq. 26 for both the low speed and high speed ranges. It can be observed that in the high speed range the direct drive spindle losses L_S are higher than in the traditional spindle system. This is mainly linked to the electric losses L_{SE}: they are close to be double if compared to the whole losses $(L_{Smg} + L_{SE})$ of the traditional spindle. This is mainly due to the control strategy used in the PMSM direct drive spindle. At low spindle speeds, on the contrary, the losses L_S observed in the traditional spindle solution are close to be double to the one of the direct drive spindle. This is surely due to the losses associated to the transmission but even more due to high electrical losses L_{SE} of the traditional spindle system. Since each spindle system has their own weak and strong points from the losses perspective, a more detailed analysis considering a realistic scenario of use is requested to infer about the two solutions.

4.3. Spindle efficiency modeling

In this Section the spindle efficiency models $\eta_S(n,T)$ were obtained using the methodology already presented in Section 4.1: experimental observations of $\eta_S(n,T)$ were first computed using Eq. 6 and then fitted with regression models. For developing the $\eta_{GS}(n,T)$ models, it was necessary to identify the parameters (Table 5) of the model reported in Eq. 14. As already anticipated, long run experimental tests were carried out for obtaining suitable data ($\overline{P_{AUXein}}(n_j,T_j)$, $\overline{L_S}(n_j,T_j)$) for the model development. It can be observed that for the gearbox based spindle, due to the presence of the oil pump and gearbox chiller, the identified model shows higher P_{AUXein_0} and m values.

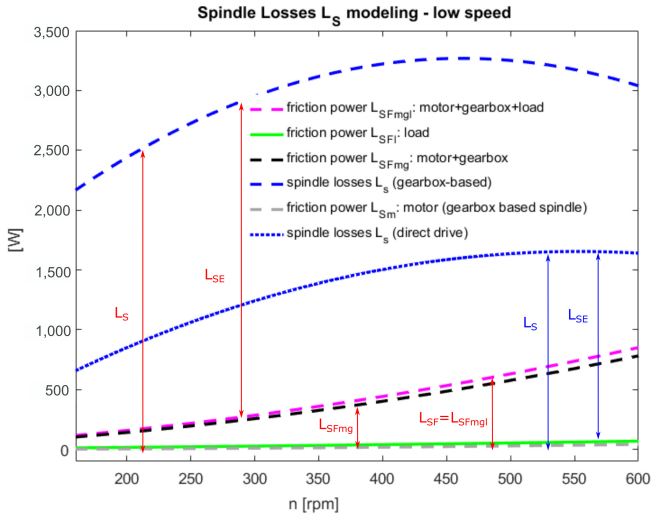

Figure 12: Spindle losses map - low speed configuration ($T = 0$)

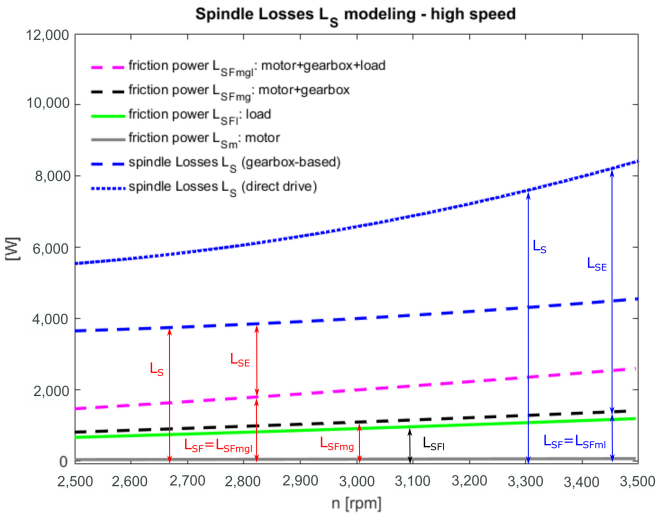

Figure 13: Spindle losses map - high speed configuration ($T = 0$)

spindle system	P_{AUXein_0} [W]	m
gearbox-based spindle	2,808	0.117
direct-drive spindle	2,162.8	0.092

Table 5: Identified parameters of the auxiliary equipment energy model

Using Eq. 13 and Eq. 14 it was possible to compute $\eta_{GS}(n, T)$ for all the tested conditions, Figure 14. The detrimental effect of the auxiliary equipment on the spindle efficiency ($\eta_S \rightarrow \eta_{GS}$) can be appreciated. It strongly depends on the analyzed spindle system, on the spindle configuration (high torque or high speed) and on the working conditions.

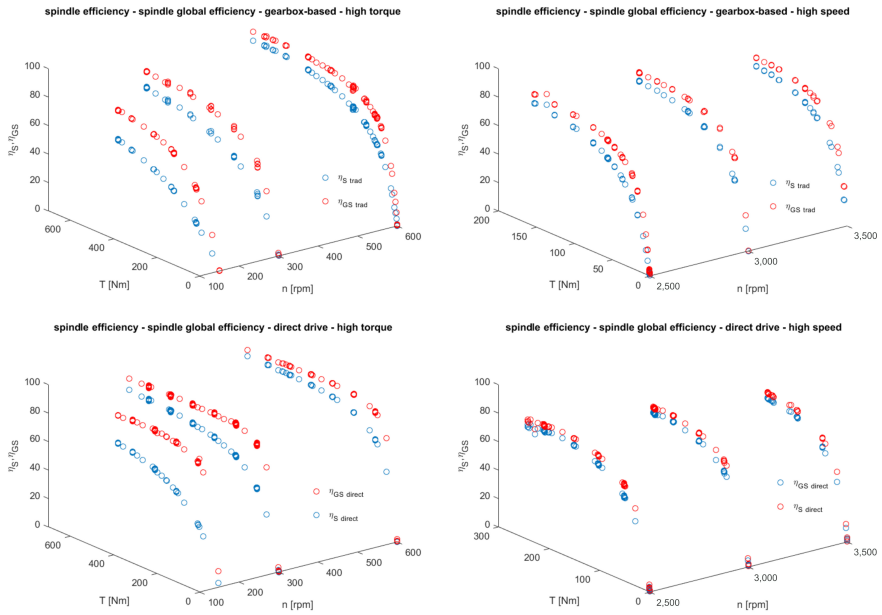

Figure 14: Spindle efficiency η_S - spindle global efficiency η_{GS} - experimental observations

Finally, a regression model was also developed for η_{GS}.

The comparison between the performance of the analyzed spindles in terms of global efficiency η_{GS} can be over-viewed in Figure 15 where the percentage difference were reported for the analyzed n and T ranges.

When the spindle works at low spindle speeds, the efficiency of the novel spindle solution η_{GS} is higher (up to 14%) than the one observed for the classical solution. This is mainly due to the energy absorbed by the pump and the gearbox chiller.

For what concerns the spindle behaviour in the high speed range, the direct drive solution exhibits a worse global efficiency η_{GS} (up to -14%) although it strongly depends on the loading conditions. This trade-off needes to be inves-

tigated.The direct drive spindle shows higher L_S but at the same time lower P_{AUX}. Such high observed motor losses L_S are intrinsically connected to the motor type used for the direct drive solution (PMSM) that needs, when the speed increases, a weakened magnetic flux. The field weakening is obtained by increasing the motor direct current i_d that is typically set at $i_d = 0$ when the motor is rotating at low spindle speeds. The i_d increment has a detrimental effect on the copper losses, Pillay and Krishnan (1989). The field weakening is a strategy that assures the reduction of the back-electromotive force (back-EMF) and consequently the prevention of the drive voltage limitation crossing, Liu (2005). Despite the high losses, the motor efficiency η_S values are within typical ranges for the considered motor type, Cavallaro et al. (2005). This demonstrates that the PMSM was properly designed for the application.

On the contrary, in order to fulfil the drive voltage limitation when the asynchronous motor AC is put into rotation at high speed, the stator phase current is reduced. This makes the spindle losses increasing less with the velocity if compared to the direct drive solution.

It is worth of noting that a trivial evaluation of the energy assessment of both the solution is not adequate. In order to tackle this issue, it was decided to estimate the potential energy savings that could be achieved with the novel direct drive solution referring to realistic machine working conditions. The results of the analysis are reported in Section 6.

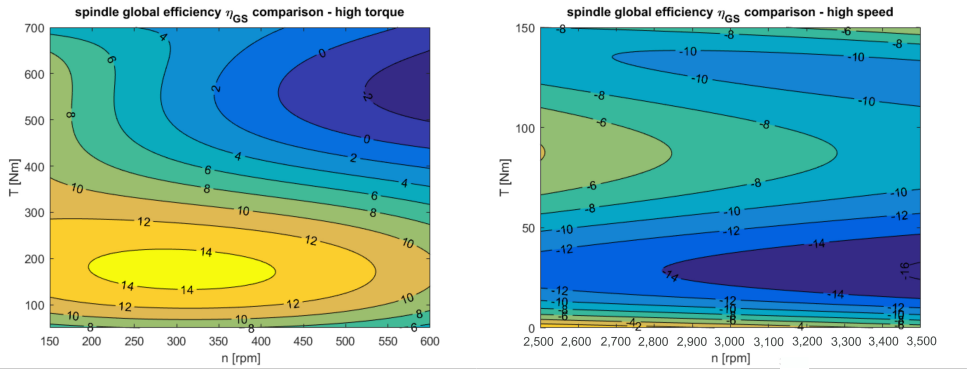

Figure 15: Spindle global efficiency η_{GS} modeling and comparison (percentage values)

5. Model Validation

In this section, the validation of the developed spindle energy model is reported. For this purpose, a real cutting test (a face milling operation) was carried out through the machine ($Jomax265$) equipped with the traditional gearbox-based spindle solution. The experimentally acquired spindle power P_{Sein} was compared to the power estimation performed through the developed model, Eq. 27. For sake of generality, it was decided to focus on a machining

operation with a not negligible contribution for what concerns the cutting power demand, P_{cutt}. More specifically, in the model validation test, a portion of machine tool (Steel $S355$) basement was machined using the tool and the cutting parameters reported in Table 6. The power absorbed by the spindle P_{Sein} was

Parameter	Value
processed material	steel $S355$
tool diameter D	160 mm
number of teeth Z	8
lead angle	90 degree
spindle speed n	600 rpm
axes feed F	1,200 mm/min
axial depth of cut a_p	2 mm
radial depth of cut a_e	120 mm

Table 6: model validation - tool and cutting conditions

estimated considering different contributions, as reported in Eq. 27.

$$P_{Sein}(n,T) = L_S(n,T) + P_{cutt} = L_{SF}(n) + L_{SE}(n,T) + P_{cutt} \qquad (27)$$

The cutting power P_{cutt} and the respective cutting torque ($T \approx 199\,Nm$), that depend on the processed material, tool properties and on cutting parameters, were estimated through the milling simulation software CutPro, (MAL, 2008). Both the friction losses L_{SF} and the electrical losses L_{SE} were estimated through the developed models and knowing the spindle working conditions in terms of n and T.

As can be observed in Figure 16, the agreement between the spindle power P_{Sein} prediction and the measured value is good. Indeed, the error in the estimation is about 2.7%. It was observed that in this specific cutting condition, the cutting power P_{cutt} accounts for the 84.2% of the spindle power P_{Sein}, the friction losses L_{SF} for the 5.7% and the electrical losses L_{SE} for the 10.1%.

The reported validation demonstrates that the developed spindle energy modeling approach can be reliably used for estimating the absorbed spindle power of real machining operations and that the model is an extremely useful instrument for performing the assessment of the energy savings presented in Section 6.

6. Energy savings evaluation and results discussion

In the presented research, it was not possible to arrange proper cutting tests using both the analysed spindle systems. Indeed, it would have requested the substitution of the traditional spindle with the direct drive one on the analyzed machining centre (Jomax265) and this would have involved unacceptable drawbacks for the company that is still using the machine for its regular production. As already described, this limitation was fully overcome performing the experimental tests on the bench that is equipped with the brakes for emulating the

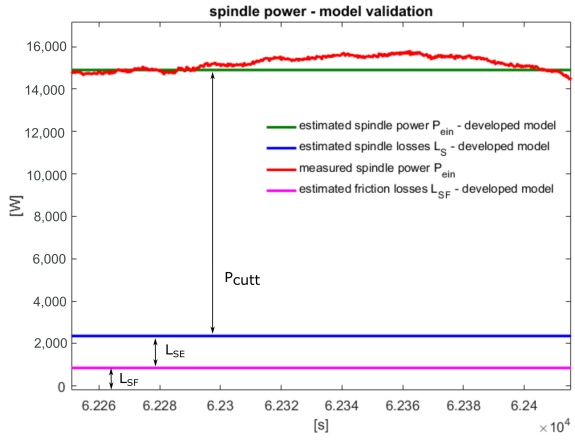

Figure 16: spindle power P_{Sein} - comparison between experimental measurement and model estimation

cutting process, section 3. This approach allowed testing and comparing both the spindles in several cutting conditions and it did not introduce any limitation or restriction for what concerns the the validity of the energy evaluation. Indeed, the power consumption comparison between the traditional and direct drive spindles was done at the net of the cutting power that was identically extracted (intended as power flow) to both the spindle systems just setting the same value of torque T (through the brake) at the same rotational speed n. In addition, for being able to compare the power consumption and the efficiency of both the spindles in any generic working condition within the tested ranges of torque and speed, suitable models were developed (section 4) and validated, section 5.

Although the results achieved in section 4 are intrinsically valuable they are not so useful because they are not contextualized from the manufacturing point of view. For this reason, a proper energy saving analysis was performed considering a realistic production scenario for the analyzed machine.

For sake of generality, in the selected reference production batch, the machine tool performed both low speed (roughing (high torque) - finishing (low torque)) operations and high speed-low torque (i.e. drilling and threading) operations. The machine was monitored for two real shifts ($T_p \simeq 16\,h$) and for each performed machining operation, the requested average spindle torque T_K, the spindle speed n_K and the duration Δt_K were gathered. Moreover, the global machine power $P_{Mein}(t)$ and the spindle power $P_{Sein}(t)$ were both experimentally measured.

The energy savings ΔE_{TOT} estimation was carried out with the support of the developed losses L_S models. As already anticipated, the comparison was done at null of the cutting power. ΔE_{TOT} was computed, as explained by Eq. 28, considering both the contribution due to the spindle ΔE_S and the one

linked to the auxiliary equipment, that is twofold: ΔE_{AUX} and ΔE_{AUX_0}. Both the terms are strictly connected to the less energy demanding cooling system used in the direct drive spindle solution. More specifically, ΔE_{AUX} represents the energy saving that can be obtained when the spindle is performing a proper cutting while ΔE_{AUX_0} is the energy saved during the ready-to-operate state.

$$\Delta E_{TOT} = \Delta E_{AUX} + \Delta E_{AUX_0} + \Delta E_S \tag{28}$$

ΔE_{AUX} was estimated using Eq. 29, where $\Delta P_{AUXein}(n_K, T_K)$ is the difference, for each machining operation, between the electric powers absorbed by the two cooling systems.

$$\Delta E_{AUX} = \sum_{K=1}^{n} \Delta E_{AUX_K} = \sum_{K=1}^{n} \Delta P_{AUXein}(n_K, T_K) \cdot \Delta t_K \tag{29}$$

As can be observed, ΔE_{AUX} depends on the considered machining operations. Such a detailed analysis was possible thanks to the developed cooling system modeling that puts into relationship the chiller power with the spindle load, Eq. 14.

ΔE_{AUX_0} was computed using Eq. 30: it does not depend on the performed machining operations but it is strictly related to the time duration T_0 the machine is in the ready-to-operate state.

$$\Delta E_{AUX_0} = \Delta P_{AUXein_0} \cdot \left(T_p - \sum_{K=1}^{n} \Delta t_K\right) = \Delta P_{AUXein_0} \cdot T_0 \tag{30}$$

For what concerns the energy savings strictly connect to the the spindle, they can be computed as reported in Eq. 31 where $\Delta L_S(n_K, T_K)$ represents the losses difference among the two alternative spindle solutions. Even in this case, ΔE_S is spindle task dependent, Figure 8.

$$\Delta E_S = \sum_{k=1}^{n} \Delta E_{S_K} = \sum_{k=1}^{n} \Delta L_S(n_K, T_K) \cdot \Delta t_K \tag{31}$$

ΔE_S is evaluated at null of the cutting power P_{cutt} that is equal for both the analyzed spindle solutions.

The reported equations were used for estimating the potential energy savings in the following situations:

- the execution of a set of machining operations (taken as the reference case) extracted from a real production batch.
- the execution of fictitious production scenarios originated from the reference case. Indeed, a sensitive analysis was performed changing some parameters in order to generalize as much as possible the results. In particular the following simulations were done

– a sensitive analysis was performed changing the durations of all the considered machining operations (Δt_K). This roughly emulated the processing of similar workpieces (same requested n_K-T_K combinations) but with different dimensions. For doing that, each Δt_K was varied up to $\pm 40\%$ as reported in Table 7. For all the simulations, the same T_0 observed in the reference case was used because it was assumed that the same amount of time is approximatively requested for setting a new workpiece in the machine.

case	high torque configuration	high velocity configuration	scenario
a	$1.4 \cdot \Delta t_K$	$1.4 \cdot \Delta t_K$	different dimensions
b	$1.2 \cdot \Delta t_K$	$1.2 \cdot \Delta t_K$	different dimensions
n	$1 \cdot \Delta t_K$	$1 \cdot \Delta t_K$	reference condition
c	$0.8 \cdot \Delta t_K$	$0.8 \cdot \Delta t_K$	different dimensions
d	$0.6 \cdot \Delta t_K$	$0.6 \cdot \Delta t_K$	different dimensions

Table 7: Sensitive analysis considering different workpiece dimensions

– Another sensitive analysis was performed considering a different balance between operations performed at low and high velocity. Even in this case, the analysis was accomplished changing the duration of each single operation as described in Table 8. The nominal T_0 was considered for all the simulated cases.

case	high torque configuration	high velocity configuration	scenario
a1	$1.4 \cdot \Delta t_K$	$0.6 \cdot \Delta t_K$	different usage
b1	$1.2 \cdot \Delta t_K$	$0.8 \cdot \Delta t_K$	different usage
n	$1 \cdot \Delta t_K$	$1 \cdot \Delta t_K$	reference condition
c1	$0.8 \cdot \Delta t_K$	$1.2 \cdot \Delta t_K$	different usage
d1	$0.6 \cdot \Delta t_K$	$1.4 \cdot \Delta t_K$	different usage
e1	$0.05 \cdot \Delta t_K$	$1 \cdot \Delta t_K$	different usage
f1	$1 \cdot \Delta t_K$	$0 \cdot \Delta t_K$	different usage

Table 8: Sensitive analysis considering a different balance between machining operations performed at low and high spindle speeds

Focusing first on reference production batch, Figure 17 shows the potential cumulated energy saving. The sequence of analyzed operations, characterized by the corresponding T_K, n_K and Δt_K, is reported on the left side of Figure 17. The energy saving contributions due to the spindle ΔE_S and due to the auxiliary equipment (ΔE_{AUX}), according to the definition reported in Eq. 28-Eq. 31, can be appreciated. It can be observed that the role of the auxiliary equipment is more relevant than the contribution due to the spindle although it positively affects the global energy saving ΔE_{TOT}. As can be easily observed looking at Figure 17, ΔE_{S_K} is positive when the machining operation is performed with the spindle set in high torque configuration while is negative when high speed

machining operations are carried out. The new conceived spindle direct solution shows a better global efficiency η_{GS} when it performs machining operation at low spindle speeds. On the contrary, when the spindle has to perform very light operations at quite high rotational speeds (i.e. threading and drilling) the spindle contribution to energy saving is negative $\Delta E_{S_K} < 0$.

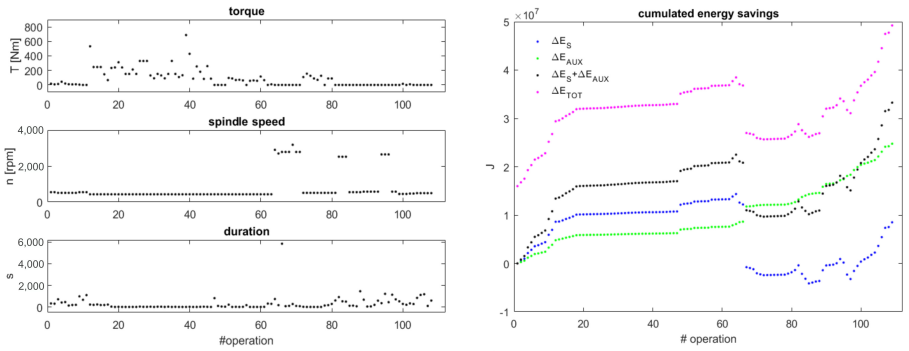

Figure 17: Composition of the reference production (T_K, n_K and Δt_K) on the left. Cumulated energy savings across the reference production execution - global ΔE_{TOT} and contributions linked to spindle ΔE_S, auxiliary equipment ΔE_{AUX} and $\Delta E_S + \Delta E_{AUX}$, on the right

Just for having an idea of energy enhancement, the energy saving percentage E_{SS-M} referred to the overall absorbed machined energy E_{Mein} and energy saving percentage E_{SS-S} referred to the absorbed spindle energy E_{Sein} were defined and computed according to Eq. 32 and Eq. 33 respectively.

$$\Delta E_{SS-M} = \frac{\Delta E_{TOT}}{E_{Mein}} = 7.4\% \tag{32}$$

E_{Mein} can be computed as done in Eq. 1 considering the experimentally measured machine power $P_{Mein}(t)$ and the production taken as the reference case.

$$\Delta E_{SS-S} = \frac{\Delta E_{TOT}}{E_{Sein}} = 63\% \tag{33}$$

E_{Sein} can be similarly computed through Eq. 2 considering the measured spindle power $P_{Sein}(t)$

Another meaningful metric is the energy saving percentage ΔE_{SS-CE}, defined with respect to the nominal cutting energy E_{CE}, Eq. 34.

$$\Delta E_{SS-CE} = \frac{\Delta E_{TOT}}{E_{CE}} = 147\% \tag{34}$$

And E_{CE} is computed through Eq. 35

$$E_{CE} = \sum_k \left(T_K \cdot n_K \cdot \frac{2\pi}{60} \cdot \Delta t_K\right) \tag{35}$$

According to the estimated energy saving indicators (ΔE_{SS-M}, ΔE_{SS-S} and ΔE_{SS-CE}) it can be concluded that considerable amount of energy can be saved with the novel direct drive spindle solution.

It is worth of noting that ΔE_{SS-CE} is more general than the previously defined indicators since it can be computed just knowing the sequence of machining operations to be executed. This property makes ΔE_{SS-CE} particularly suitable for performing the describes sensitive analyzes. The obtained results are reported in Figure 18 and Figure 19.

Focusing first on Figure 18, it can be noted that ΔE_{SS-CE} increases with the decrement of the operation durations. What observed is due to a less relevant reduction of ΔE_{TOT} if compared to the one registered for E_{CE}. This depends on the fact that ΔE_{AUX_0} is kept constant.

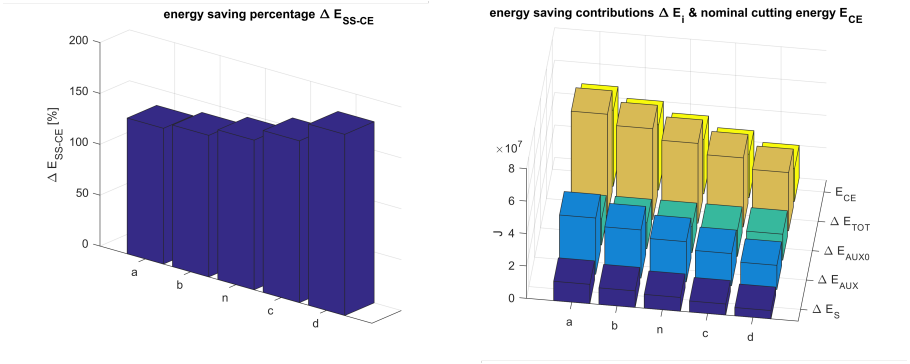

Figure 18: Sensitive analysis. Workpiece dimensions effect. Energy saving percentage Delta E_{SS-CE} on the left, energy savings contributions ΔE_i and nominal cutting energy E_{CE} on the right

Similarity, the results of the other sensitive analysis are reported in Figure 19. It shows how ΔE_{SS-CE} and the energy saving contributions vary if a generic workpiece requires more machining operations performed at low spindle speed or vice-versa. The cases reported in Table 8 were simulated.

It can be observed that if the workpiece processing needs more light machining operations performed at high spindle speeds, the ΔE_{SS-CE} tends to decrease. $\Delta E_{SS-CE} \simeq 105\%$ in the "d1" case. While using such a multifunctional machine just for drilling and threading would be highly unlikely, the "e1" case was analyzed. In this test case the machining operations performed at low spindle speeds are reduced of the 95%.

The simulation results show that ΔE_{SS-CE} is almost vanished. More in details, the energy savings strictly connected to the spindle ΔE_S moved to a negative value even if it is compensated by both ΔE_{AUX_0} and ΔE_{AUX}. This is the most critical spindle working condition for what concerns the exploitation of the potential energy savings connected to the use of the direct drive solution. On the contrary, if operations at low spindle speeds ("f1" case with roughing and finishing) are mainly performed, the energy savings can be considerable

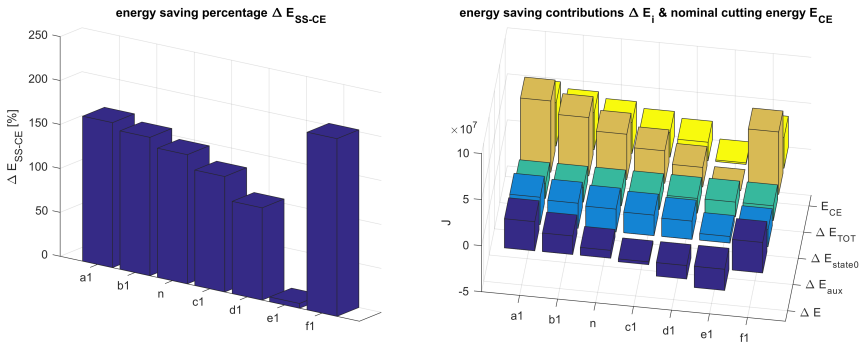

Figure 19: Sensitive analysis. Effects of different balances between low-high speed operations. Energy saving percentage Delta E_{SS-CE} on the left, energy savings contributions ΔE_i and nominal cutting energy E_{CE} on the right

($\Delta E_{SS-CE} \simeq 202\%$) high. For the analyzed machine, production scenarios ascribable to "a1", "b1" or "f1" cases are surely more realistic. The performed additional analyses confirm the energy savings potentialities of the direct drive technology in spindle system design.

7. Conclusions

The potentialities, in terms of energy savings, of a spindle direct drive solution for a multi-functional machine centre were investigated. The energy assessment was carried out with respect to a traditional spindle solution based on a gearbox that assures the possibility of executing both high torque–low speed and low torque–high speed machining operations.

A combined experimental-modeling procedure was opportunely conceived for performing this analysis. Both the spindle systems, together with the linked auxiliary equipment, were tested on a specific bench equipped with brakes in order to simulate real cutting conditions. The experimental data were used for developing energy models (losses L_S, spindle efficiency η_S and spindle system global efficiency η_{GS}) of the two spindle solutions.

A comprehensive energy assessment was carried out with the support of the developed models and defining a realistic scenario of use for the considered machine. More specifically, a set of many real machining operations was used for comparing the energy consumed by the alternative spindle systems. The energy analysis showed that considerable amount of energy can be saved substituting the traditional spindle with the novel direct drive solution. It was estimated that, for the considered reference production batch, up to 7% of the overall machine tool energy consumption can be saved. This amount of saved energy corresponds to the $\Delta E_{SS-CE} = 147\%$ of the requested cutting energy. The analysis was also extended simulating other hypothetical production scenarios. For instance, this percentage ΔE_{SS-CE} ranges from 133% to 178% just changing the duration of each analyzed machining operation. Since it was found

that the direct drive solution, for what purely concerns the electrical motor losses in the high spindle speed range, is less efficient than the classical solution, a second sensitive analysis was specifically conceived to study this potential critical aspect. The analysis was performed changing, in the set of machining operations used as a reference, the balance between roughing operations (high torque demanding) and the machining operations performed at high speeds (i.e. threading, drilling and finishing). The results showed that, even in the extreme and rather unlikely case in which most of the performed machining operations are finishing operations, the energy saving still remains positive even if the enhancement is practically negligible. The reported analysis does not only confirm the extremely positive impact of the direct drive spindle solution on the overall energy consumed by the machine but also shows that the achievable energy savings are quite robust to changes to the way the machine is used.

Acknowledgement

The EROD project was been funded by the Italian Ministry of Economic Development within the Industria 2015 Programme, Energy Efficiency, which involves 20 partners from Academia, Research and industry. The author would thank Eng. Mapelli, Tarsitano, Apuzzo, Solari for their contributions to the experimental tests session.

References

Abele, E., Altintas, Y., Brecher, C., 2010. Machine tool spindle units. CIRP Annals - Manufacturing Technology 59, 781 – 802. doi:10.1016/j.cirp.2010.05.002.

Abele, E., Sielaff, T., Schiffler, A., Rothenbücher, S., 2011. Analyzing Energy Consumption of Machine Tool Spindle Units and Identification of Potential for Improvements of Efficiency. Springer Berlin Heidelberg, Berlin, Heidelberg. pp. 280–285. doi:10.1007/978-3-642-19692-8_49.

Albertelli, P., Keshari, A., Matta, A., 2016. Energy oriented multi cutting parameter optimization in face milling. Journal of Cleaner Production 137, 1602 – 1618. doi:10.1016/j.jclepro.2016.04.012.

Altıntaş, R.S., Kahya, M., Ünver, H.Ö., 2016. Modelling and optimization of energy consumption for feature based milling. The International Journal of Advanced Manufacturing Technology 86, 3345–3363. doi:10.1007/s00170-016-8441-7.

Aramcharoen, A., Mativenga, P.T., 2014. Critical factors in energy demand modelling for cnc milling and impact of toolpath strategy. Journal of Cleaner Production 78, 63 – 74. doi:10.1016/j.jclepro.2014.04.065.

Avram, O.I., Xirouchakis, P., 2011. Evaluating the use phase energy requirements of a machine tool system. Journal of Cleaner Production 19, 699 – 711. doi:10.1016/j.jclepro.2010.10.010.

Balogun, V.A., Mativenga, P.T., 2013. Modelling of direct energy requirements in mechanical machining processes. Journal of Cleaner Production 41, 179 – 186. doi:10.1016/j.jclepro.2012.10.015.

Boglietli, A., Cavagnino, A., Lazzari, M., Pastorelli, A., 2003. Induction motor efficiency measurements in accordance to ieee 112-b, iec 34-2 and jec 37 international standards, in: Electric Machines and Drives Conference, 2003. IEMDC'03. IEEE International, pp. 1599–1605 vol.3. doi:10.1109/IEMDC.2003.1210664.

Borgia, S., Albertelli, P., Bianchi, G., 2016. A simulation approach for predicting energy use during general milling operations. The International Journal of Advanced Manufacturing Technology , 1–15doi:10.1007/s00170-016-9654-5.

Bossmanns, B., Tu, J., 2001. A power flow model for high speed motorized spindlesheat generation characterization. Transaction of ASME 123, 494–505.

Bossmanns, B., Tu, J.F., 1999. A thermal model for high speed motorized spindles. International Journal of Machine Tools and Manufacture 39, 1345 – 1366. doi:10.1016/S0890-6955(99)00005-X.

Brecher, C., Bäumler, S., Jasper, D., Triebs, J., 2012. Energy Efficient Cooling Systems for Machine Tools. Springer Berlin Heidelberg, Berlin, Heidelberg. pp. 239–244. doi:10.1007/978-3-642-29069-5_41.

Brecher, C., Jasper, D., Fey, M., 2017. Analysis of new, energy-efficient hydraulic unit for machine tools. International Journal of Precision Engineering and Manufacturing-Green Technology 4, 5–11. doi:10.1007/s40684-017-0001-6.

Calvanese, M., Albertelli, P., Matta, A., Taisch, M., 2013. Analysis of energy consumption in cnc machining centers and determination of optimal cutting conditions, in: Re-engineering Manufacturing for Sustainability, pp. 227–232.

Campatelli, G., Lorenzini, L., Scippa, A., 2014. Optimization of process parameters using a response surface method for minimizing power consumption in the milling of carbon steel. Journal of Cleaner Production 66, 309 – 316. doi:10.1016/j.jclepro.2013.10.025.

Cavallaro, C., Tommaso, A.O.D., Miceli, R., Raciti, A., Galluzzo, G.R., Trapanese, M., 2005. Efficiency enhancement of permanent-magnet synchronous motor drives by online loss minimization approaches. IEEE Transactions on Industrial Electronics 52, 1153–1160. doi:10.1109/TIE.2005.851595.

CECIMO, 2009. Self-regulation initiative. URL: www.cecimo.eu/site/ecodesign-and-self-regulatory-initiative/self-regulation-for-machine-tools/. (Date last accessed 2016-12-21).

Diaz, N., Helu, M., Jarvis, A., Tnissen, S., Dornfeld, D., Schlosser, R., 2009. Strategies for minimum energy operation for precision machining. The Proceedings of MTTRF Annual Meeting.

Draganescu, F., Gheorghe, M., Doicin, C., 2003. Models of machine tool efficiency and specific consumed energy. Journal of Materials Processing Technology 141, 9 – 15. doi:10.1016/S0924-0136(02)00930-5.

EU, 2009. Ecodesign requirements for energy-related products erp directive 2009/125/ec. Official Journal of the European Union 285, 10–35. URL: eur-lex.europa.eu/legal-content/EN/TXT/PDF/?uri=CELEX:32009L0125&from=EN. (Date accessed time 2016-12-21).

Fraunhofer-IZM, 2011. Energy-using product group analysis - lot 5 machine tools and related machinery. URL: www.ecomachinetools.eu/typo/home.html. (Date last accessed 2016-12-21).

Gtze, U., Koriath, H.J., Kolesnikov, A., Lindner, R., Paetzold, J., 2012. Integrated methodology for the evaluation of the energy- and cost-effectiveness of machine tools. CIRP Journal of Manufacturing Science and Technology 5, 151 – 163. doi:10.1016/j.cirpj.2012.04.001.

Guo, Y., Duflou, J.R., Qian, J., Tang, H., Lauwers, B., 2015. An operation-mode based simulation approach to enhance the energy conservation of machine tools. Journal of Cleaner Production 101, 348 – 359. doi:10.1016/j.jclepro.2015.03.097.

Gutowski, T., Dahmus, J., Thiriez, J., 2006. Electrical energy requirements for manufacturing processes., in: 13th CIRP International Conference of Life Cycle Engineering, Lueven, Belgium.

Hanafi, I., Khamlichi, A., Cabrera, F.M., Almansa, E., Jabbouri, A., 2012. Optimization of cutting conditions for sustainable machining of peek-cf30 using tin tools. Journal of Cleaner Production 33, 1 – 9. doi:10.1016/j.jclepro.2012.05.005.

Harris, P., Linke, B., Spence, S., 2015. An energy analysis of electric and pneumatic ultra-high speed machine tool spindles. Procedia CIRP 29, 239 – 244. doi:10.1016/j.procir.2015.02.046.

He, Y., Liu, F., Wu, T., Zhong, F.P., Peng, B., 2012. Analysis and estimation of energy consumption for numerical control machining. Proceedings of the Institution of Mechanical Engineers, Part B: Journal of Engineering Manufacture 226, 255–266. doi:10.1177/0954405411417673.

Huang, H., Ameta, G., 2014. Computational energy estimation tools for machining operations during preliminary design. International Journal of Sustainable Engineering 7, 130–143. doi:10.1080/19397038.2013.862580.

ISO, 2014. 14955-1 machine tools - environmental evaluation of machine tools - part 1: Design methodology for energy-efficient machine tools. URL: www.iso.org/iso/home/store/catalogue_tc/catalogue_detail.htm?csnumber=70035. (Date last accessed 2016-12-21).

ISO, 2016. 14955-2 machine tools - environmental evaluation of machine tools – part 2: Methods for measuring energy supplied to machine tools and machine tool components. URL: www.iso.org/iso/home/store/catalogue_tc/catalogue_detail.htm?csnumber=66354. (Date last accessed 2016-12-29).

Jayal, A., Badurdeen, F., Jr., O.D., Jawahir, I., 2010. Sustainable manufacturing: Modeling and optimization challenges at the product, process and system levels. CIRP Journal of Manufacturing Science and Technology 2, 144 – 152. doi:10.1016/j.cirpj.2010.03.006.

Jimoh, A.A., Findlay, R.D., Poloujadoff, M., 1985. Stray losses in induction machines: Part i, definition, origin and measurement. IEEE Transactions on Power Apparatus and Systems PAS-104, 1500–1505. doi:10.1109/TPAS.1985.319165.

Kant, G., Sangwan, K.S., 2014. Prediction and optimization of machining parameters for minimizing power consumption and surface roughness in machining. Journal of Cleaner Production 83, 151 – 164. doi:10.1016/j.jclepro.2014.07.073.

Kara, S., Li, W., 2011. Unit process energy consumption models for material removal processes. CIRP Annals - Manufacturing Technology 60, 37 – 40. doi:10.1016/j.cirp.2011.03.018.

Li, J.g., Lu, Y., Zhao, H., Li, P., Yao, Y.x., 2014. Optimization of cutting parameters for energy saving. The International Journal of Advanced Manufacturing Technology 70, 117–124. doi:10.1007/s00170-013-5227-z.

Li, L., Yan, J., Xing, Z., 2013. Energy requirements evaluation of milling machines based on thermalequilibrium and empirical modelling. Journal of Cleaner Production 52, 113 – 121. doi:10.1016/j.jclepro.2013.02.039.

Li, W., Zein, A., Kara, S., Herrmann, C., 2011. An Investigation into Fixed Energy Consumption of Machine Tools. Springer Berlin Heidelberg, Berlin, Heidelberg. pp. 268–273. doi:10.1007/978-3-642-19692-8_47.

Liu, Q., 2005. Analysis, design and control of permanent magnet synchronous motors for wide-speed operation. Ph.D. thesis. National University of Singapore.

MAL, 2008. Cut pro simulation sofware. URL: www.malinc.com/products/cutpro/. (Date last accessed 2017-05-17).

Mativenga, P., Rajemi, M., 2011. Calculation of optimum cutting parameters based on minimum energy footprint. CIRP Annals - Manufacturing Technology 60, 149 – 152. doi:10.1016/j.cirp.2011.03.088.

Montgomery, D.C., 2001. Design of Experiments. John Wiley.

Neugebauer, R., Wabner, M., Rentzsch, H., Ihlenfeldt, S., 2011. Structure principles of energy efficient machine tools. CIRP Journal of Manufacturing Science and Technology 4, 136 – 147. doi:10.1016/j.cirpj.2011.06.017. energy-Efficient Product and Process Innovations in Production Engineering.

Newman, S., Nassehi, A., Imani-Asrai, R., Dhokia, V., 2012. Energy efficient process planning for cnc machining. CIRP Journal of Manufacturing Science and Technology 5, 127 – 136. doi:10.1016/j.cirpj.2012.03.007.

Pavanaskar, S., Pande, S., Kwon, Y., Hu, Z., Sheffer, A., McMains, S., 2015. Energy-efficient vector field based toolpaths for cnc pocketmachining. Journal of Manufacturing Processes 20, Part 1, 314 – 320. doi:10.1016/j.jmapro.2015.06.009.

Pillay, P., Krishnan, R., 1989. Modeling, simulation, and analysis of permanent-magnet motor drives. i. the permanent-magnet synchronous motor drive. IEEE Transactions on Industry Applications 25, 265–273. doi:10.1109/28.25541.

Rahman, M.A., Zhou, P., 1996. Analysis of brushless permanent magnet synchronous motors. IEEE Transactions on Industrial Electronics 43, 256–267. doi:10.1109/41.491349.

Rajemi, M., Mativenga, P., Aramcharoen, A., 2010. Sustainable machining: selection of optimum turning conditions based on minimum energy considerations. Journal of Cleaner Production 18, 1059 – 1065. doi:10.1016/j.jclepro.2010.01.025.

Sizov, G.Y., Ionel, D.M., Demerdash, N.A.O., 2012. Modeling and parametric design of permanent-magnet ac machines using computationally efficient finite-element analysis. IEEE Transactions on Industrial Electronics 59, 2403–2413. doi:10.1109/TIE.2011.2163912.

Velchev, S., Kolev, I., Ivanov, K., Gechevski, S., 2014. Empirical models for specific energy consumption and optimization of cutting parameters for minimizing energy consumption during turning. Journal of Cleaner Production 80, 139 – 149. doi:10.1016/j.jclepro.2014.05.099.

Wang, Q., Liu, F., Wang, X., 2014. Multi-objective optimization of machining parameters considering energy consumption. The International Journal of Advanced Manufacturing Technology 71, 1133–1142. doi:10.1007/s00170-013-5547-z.

Yan, J., Li, L., 2013. Multi-objective optimization of milling parameters the trade-offs between energy, production rate and cutting quality. Journal of Cleaner Production 52, 462 – 471. doi:10.1016/j.jclepro.2013.02.030.

Yang, Y., Li, X., Gao, L., Shao, X., 2016. Modeling and impact factors analyzing of energy consumption in cnc face milling using grasp gene expression programming. The International Journal of Advanced Manufacturing Technology 87, 1247–1263. doi:10.1007/s00170-013-5017-7.

Yi, Q., Li, C., Tang, Y., Chen, X., 2015. Multi-objective parameter optimization of cnc machining for low carbon manufacturing. Journal of Cleaner Production 95, 256 – 264. doi:10.1016/j.jclepro.2015.02.076.

Yingjie, Z., 2014. Energy efficiency techniques in machining process: a review. The International Journal of Advanced Manufacturing Technology 71, 1123–1132. doi:10.1007/s00170-013-5551-3.

Zhou, L., Li, J., Li, F., Meng, Q., Li, J., Xu, X., 2016. Energy consumption model and energy efficiency of machine tools: a comprehensive literature review. Journal of Cleaner Production 112, Part 5, 3721 – 3734. doi:10.1016/j.jclepro.2015.05.093.